BSc thesis APPLIED MATHEMATICS & APPLIED PHYSICS

"Noiseless clusters and perturbations in networks of coupled quantum harmonic oscillators"

JORIS VAN WINDEN

Delft University of Technology

Supervisors

Dr. J.L.A Dubbeldam

Dr. T.H. Taminiau

Comittee members

Dr. B. Janssens

Dr. A.R. Akhmerov

August, 2020

Delft

Abstract

In this thesis, networks of coupled quantum harmonic oscillators are studied. The dynamics of these networks are determined by single-frequency vibrations of the entire network called normal modes. We study the behavior of the normal modes when the network is coupled to a thermodynamical heat bath by looking at the Lindblad Master Equation of the system. From this equation, we determine the rate at which the normal modes decay. Certain normal modes decay very slowly, and some do not decay at all. These normal modes are called quasi-noiseless and noiseless clusters respectively.

We determine what happens to the noiseless clusters when the network parameters are very slightly perturbed. We have found that two distinct types of noiseless clusters can be identified. The first type disappears with even the slightest perturbation, making it useless in practice. The second type instead becomes quasi-noiseless, making it a viable candidate for applications. We show how to determine the degree to which these noiseless clusters become quasi-noiseless by looking at the other normal modes of the network.

We also explain how a network of oscillators, including an optional heat bath, can be simulated with an optical setup as described in [3]. We suggest this setup can be used to verify our findings.

Contents

1 Introduction

The harmonic oscillator is one of the simplest physical systems with interesting dynamics. Despite its elegant simplicity it shows up in many different situations, from a simple mass on a spring to the vibrations of atoms in a lattice. In fact, particle physicist Michael Peskin is said to have stated that "Physics is that subset of human experience which can be reduced to coupled harmonic oscillators." It is no wonder then that the quantum mechanical version of this system has been extensively studied. In this thesis, we study the dynamics of networks of coupled quantum harmonic oscillators.

In their paper 'Synchronization, quantum correlations and entanglement in oscillator networks', Manzano et. al. [2] demonstrated that these networks show interesting behavior when introduced to a thermodynamical environment. Specifically, they show that some vibrations in the network decay slower than others, which can lead to synchronization. Furthermore, some vibrations do not decay at all! These vibrations are called noiseless clusters. Noiseless clusters are a specific instance of decoherence-free subspaces, which are essential to produce long-lived optical states which can be used for quantum memory.

We study the occurrence of these noiseless clusters in networks which are randomly generated. Our focus lies on what happens to noiseless clusters when the network is slightly perturbed.

First, we explain the theoretical background behind network of quantum harmonic oscillators. This includes the dynamics of the oscillators, the generation of the random network, and some results from the perturbation theory of eigenvalue problems. We also explain how symmetry can affect the occurence of noiseless clusters, and describe an optical setup due to Nokkola et. al. [3] with which a quantum network of oscillators can be simulated. After that, we examine how noiseless clusters behave when the network is perturbed. We identify two types of noiseless clusters: *degenerate* and *sporadic*, and look at their qualitative differences. For a given noiseless cluster, it is possible to determine what its type is by looking at the other normal modes in the network.

We find that the degenerate clusters vanish without a trace when even the slightest perturbation is present in the network. On the other hand, the sporadic clusters are well-behaved: they become quasi-noiseless when the network is perturbed. We derive an equation which describes exactly how quasi-noiseless they become.

This thesis is part of the bachelor programs Applied Physics and Applied Mathematics at the Delft University of Technology.

2 Theoretical background

In this section, the theoretical background required for the rest of the thesis is laid out. First, the harmonic oscillator is introduced. We then transition to the quantum mechanical version of the harmonic oscillator. After that, we explain the dynamics of a network of coupled quantum harmonic oscillators, as well as their behaviour when introduced to a thermodynamical environment. Then we introduce the concept of a noiseless cluster. We then briefly summarize how a system of oscillators can be simulated with an optical setup, as described by Nokkola et. al. [3] Next, we introduce the Erdös-Renyi model of random networks, and explain how such a network can be interpreted as a network of oscillators. We also discuss how noiseless clusters arise when symmetry is present in the network. Finally, we state some theorems from the perturbation theory of eigenvalue problems, which are required for some of our results.

We assume that the reader has a basic working knowledge of linear algebra, ordinary differential equations, probability theory, abstract algebra and quantum mechanics.

2.1 Oscillators and their dynamics

2.1.1 Classical harmonic oscillators

The harmonic oscillator is one of the most fundamental physical systems. It can be described in several (equivalent) ways, one of which is following differential equation:

$$\ddot{x}(t) = -ax(t) \tag{1}$$

where a is some constant. The reason this system is called a harmonic oscillator is because the general solution to the equation is $x(t) = A\sin(\sqrt{a}t + \phi)$, where A and ϕ are constants determined by the initial conditions. $x(t)$ is just a sine wave, so it is described by harmonic motion.

This differential equation frequently arises when looking at the motion of some object when it is nearly at equilibrium. Consider a particle with mass m in some potential $V(x)$, and assume that V has a local minimum at the origin If we furthermore assume that the particle always remains very close to the origin, the potential in this region can be a approximated by the first few terms of its Taylor series.

$$V(x) \approx V(0) + xV'(0) + \frac{1}{2}x^2V''(0) \tag{2}$$

Since 0 is a local minimum of V, $V'(0)$ must be 0. We are then left with the quadratic potential $V(x) \approx V(0) + \frac{1}{2}x^2V''(0)$. Using Newton's second law, we get differential equation (1) with $a = \frac{V''(0)}{m}$.

The above derivation is very general, and implies that every system sufficiently close to equilibrium can be approximated by a harmonic oscillator.

In this thesis, we concern ourselves mainly with the quantum mechanical version of such systems. Therefore from now on, the terms '*quantum harmonics oscillator*', '*harmonic oscillator*' and '*oscillator*' are used interchangeably, and all refer to the quantum mechanical version.

2.1.2 One-dimensional Quantum Harmonic Oscillators

The one-dimensional quantum harmonic oscillator is described by a quadratic potential, conveniently centered at the origin. If we describe this system in Cartesian coordinates, the Hamiltonian takes the following form [9].

$$\hat{H} = -\frac{\hbar^2}{2m}\frac{\partial^2}{\partial x^2} + \frac{1}{2}\omega^2 m x^2 \tag{3}$$

The constant ω is referred to as the frequency of the oscillator. The Schrödinger equation for this Hamiltonian can be solved exactly, which results in the energy levels

$$E_n = \hbar\omega(n + 1/2) \tag{4}$$

where n is nonnegative positive integer.

2.1.3 Higher-dimensional Oscillators and Multiple oscillators

Now we consider an N-dimensional quantum harmonics oscillator. We use the Cartesian coordinates $x_1, x_2, ...x_N$. The potential is still quadratic in all the coordinates, which results in the following Hamiltonian.

$$\hat{H} = \sum_{i=1}^{N} -\frac{\hbar^2}{2m}\frac{\partial^2}{\partial x_i^2} + \frac{1}{2}\omega^2 m x_i^2 \tag{5}$$

From this equation we see that we can write $\hat{H}$ as the sum of the Hamiltonians of N independent one-dimensional oscillators. Since there are no cross-terms, this means that one N-dimensional quantum harmonics oscillator is equivalent to a system of uncoupled N one-dimensional oscillators. Therefore, the energies are now given by

$$E_{n_1,n_2,...n_N} = \hbar\omega(\sum_{i=1}^{N} n_i + 1/2) \tag{6}$$

where every n_i is a nonnegative integer.

Comparing equations (4) and (6) we see that the allowed energies are exactly the same. However, all energies except the ground state of the N-dimensional oscillator are degenerate, since there are many ways for N nonnegative integers to sum up to the same result. For example if we take $N = 2$ and describe the states as a two-tuple (n_1, n_2), the states $(1, 1)$, $(2, 0)$, $(0, 2)$ all have energy $5/2\hbar\omega$.

2.1.4 Coupled oscillators

Going one step further, we can consider a system of oscillators and add linear interaction terms to (5) to make couplings between the oscillators. Note that here we interpret (5) as N independent uncoupled oscillators instead of one N-dimensional oscillator. These interaction terms take the form $-\lambda_{ij}x_ix_j$, where λ_{ij} is strictly positive.

Since our system only consists of terms like x_i^2 and x_ix_j, we can write the potential as a quadratic form. Writing $x = (x_1, x_2, ..., x_N)^T$, we can see that

$$V(x_1, ..., x_N) = \frac{1}{2}x^\top Mx \tag{7}$$

where $M_{ii} = m\omega^2$, and $M_{ij} = M_{ji} = -\lambda_{ij}$. We will almost exclusively use this description of the system. Any system of linearly coupled harmonic oscillators has a matrix M, and any symmetric matrix M defines a system of linearly coupled harmonic oscillators. From now on, we will call M the *network matrix* of the system.

A convenient feature of this way of writing V is that M is symmetrical by construction. Combining this potential with the momentum term written as a vector, we get the following Hamiltonian.

$$\hat{H} = \frac{1}{2m}p^\top p + \frac{1}{2}x^\top Mx \tag{8}$$

This way of writing $\hat{H}$ makes it possible to elegantly solve the dynamics of the system by a change of variables. Since M is real symmetric, let Q be an orthogonal matrix for which $D = Q^\top MQ$ is diagonal (the fact that such a Q exists is a well-known result from linear algebra [10]). Then change variables to $x = QX$ and $p = QP$. This results in

$$\begin{aligned}\hat{H} &= \frac{1}{2m}(QP)^\top(QP) + \frac{1}{2}(QX)^\top M(QX)\\ &= \frac{1}{2m}P^\top(Q^\top Q)P + \frac{1}{2}X^\top(Q^\top MQ)X\\ &= \frac{1}{2m}P^\top P + \frac{1}{2}X^\top DX\end{aligned}$$

because of the properties of Q. Since D is diagonal, the new Hamiltonian describes n uncoupled harmonic oscillators. These uncoupled oscillations in the network are called normal modes, and their frequencies are determined by the eigenvalues of M, which are encoded in D.

From now on, we use the term 'normal mode basis' when writing equations using the X and P variables, and the term 'standard basis' when writing equations with the x and p variables.

2.1.5 Heat Bath of Oscillators

Now we examine a system of oscillators coupled to a common heat bath. We construct the heat bath and system-bath interactions as in [2]. To construct this system, we begin with the hamiltonian of the bath itself. Our bath consists of infinitely many uncoupled oscillators, which are described by the following Hamiltonian.

$$\hat{H}_B = \frac{1}{2}\sum_{j=1}^{\infty}(\frac{\mathbb{P}_j^2}{M_j} + s_j\mathbb{X}_j^2) \tag{9}$$

Here $\mathbb{X}_j$ and $\mathbb{P}_j$ are the position and momentum operators of the j-th oscillator. M_j and s_j represent the mass and the 'spring constant' of the oscillator.

The interaction between the system and the bath is modelled by linearly coupling (as in section 2.1.4) the network oscillators to the bath oscillators. Each bath oscillator gets a parameter λ_i which determines how strongly it interacts with the network. γ determines the overall strength of the couplings. In this model, all the network oscillator couple equally strong to a given bath oscillator. The system-bath interaction Hamiltonian is

$$H_{sb} = -\sqrt{\gamma}\sum_{j=1}^{\infty}\lambda_j\mathbb{X}_j(\sum_{i=1}^{n}x_i) \tag{10}$$

which can be rewritten by changing the order of summation to

$$H_{sb} = -\sum_{i=1}^{n}x_i\hat{B} \tag{11}$$

where $\hat{B} = \sqrt{\gamma}\sum_{j=1}^{\infty}\lambda_j\mathbb{X}_j$. In equation (11), we see from the symmetry in the x_i's that every node in the network is coupled equally strong to the bath. However, this is not true for the normal modes, as can be seen by changing to the normal mode coordinates X and P. In these coordinates, $x = QX$ and therefore $x_i = \sum_{j=1}^{n}Q_{ij}X_j$. Hence, the system-bath interaction Hamiltonian is:

$$H_{sb} = -\sum_{i=1}^{n}(\sum_{j=1}^{n}Q_{ij}X_j)\hat{B} \tag{12}$$

After changing the order of summation and rearranging the terms, we get:

$$H_{sb} = -\sum_{j=1}^{n}X_j(\sum_{i=1}^{n}Q_{ij})\hat{B} \tag{13}$$

Equation (13) tells us that the strength of the coupling between the j-th normal mode and the bath is determined by $k_j = \sum_{i=1}^{n}Q_{ij}$. This fact was first noted by Manzano et al. in [2]. k_j is equal to the inner product of the j-th normal mode with the center of mass coordinate, $x_{cm} = \sum_{i=1}^{n}x_n$. From now on, we

will call x_{cm} the 'dissipative mode' (even when it is not a normal mode), and we will call k_j the 'overlap with the dissipative mode'. k_j is also equal to the sum of the coefficients of the (normalized) normal mode vector in the standard basis.

Remarkably, when $k_j = 0$, the normal mode is not coupled to the heat bath at all. This has important consequences for the dynamics of the system.

2.1.6 Dissipation

Now that we have described the Hamiltonians of the system, the bath, and their interaction, it is possible to describe how dissipation occurs. Since the quantum heat bath represents the thermodynamical environment of the system, its state is fully unknown. On the other hand, the initial conditions of the system are within our control. But since the system and the bath evolve together, our ignorance about the state of the environment 'infects' the system.

To be able to describe uncertainty about the quantum state of a system, density matrices were invented. Note that this is not the same uncertainty as in Heisenberg's principle. 'Normal' quantum uncertainty says something about the measurements performed on a (in theory completely known) wavefunction. In the density matrix formalism, the state of the quantum system itself is modelled probabilistically. The system is said to be in a mixed state rather than a pure state.

The density matrix is defined as follows:

$$\rho = \sum_i p_i |\psi_i\rangle\langle\psi_i| \tag{14}$$

In this equation, i is an index which ranges over the possible states of the system (after choosing an orthonormal basis). p_i represents the (classical) probability that the system is in the state $|\psi_i\rangle$. We can contrast equation (14) to the way in which the state of a quantum mechanical system can be described as a linear combination of basis states.

$$\psi = \sum_i a_i |\psi_i\rangle \tag{15}$$

where $|a_i|^2$ is the probability that, if measured, the system will collapse to state $|\psi_i\rangle$.

When the system states is described as $|\psi\rangle$, the evolution is the system is governed by the Schrödinger equation [9].

$$\frac{\partial}{\partial t}|\psi\rangle = -\frac{\hbar}{i} H|\psi\rangle \tag{16}$$

Similarly, as can be straightforwardly derived by using the Schrödinger equation, the density matrix evolves with the von Neumann equation:

$$\frac{d}{dt}\rho = -\frac{i}{\hbar}[H, \rho] \tag{17}$$

where $[\cdot, \cdot]$ denotes the commutator bracket.

Now we must consider our network of oscillators as a subsystem of a larger (closed) system, which includes the heat bath. Since the state of the environment is in principle completely unknown, it is no easy feat to determine the evolution of our subsystem. It is possible to derive a Lindblad master equation for this system, which approximates the dynamics of the subsystem when certain assumptions hold. The derivation of this equation is beyond the scope of this thesis, and we refer to [2] for more information.

$$\begin{aligned}\frac{d\rho(t)}{dt} =& -i[H_s, \rho] \\ &- \frac{i}{4}\sum_{n=1}^{N}\Gamma_n([Q_n, \{P_n, \rho\}] - [P_n, \{Q_n, \rho\}]) \\ &- \frac{1}{4}\sum_{n=1}^{N} D_n([Q_n, [Q_n, \rho]]) - \frac{1}{\Omega^2}[P_n, [P_n, \rho]])\end{aligned} \tag{18}$$

In this equation, $\hbar$ is set to 1, the curly brackets are anticommutators ($\{a, b\} = ab + ba$), $\Gamma_n = \gamma k_n^2$, and $D_n = \frac{\gamma k_n^2 \Omega_n}{\tan(\Omega_n / 2k_B T)}$. Q_n and P_n are the position and momentum operators of the n-th normal mode, respectively. Ω_n is the eigenfrequency of the n-th normal mode.

The validity of equation (18) depends on the following assumptions [15]. Firstly, the coupling between the system nodes and the bath nodes is weak compared to the couplings of the system nodes to each other. Secondly, we assume the system state and the bath state are at all times uncorrelated. This is a unrealistic assumption in physical systems, but it can be justified as an approximation if the correlations between the system and the bath are weak and short-lived [15]. Thirdly, the environment at $t = 0$ is assumed to be in thermal equilibrium. The final approximation required is the *rotating wave approximation*. In this approximation, terms which oscillate much faster than the system as a whole are neglected. There is also the implicit assumption that the system evolution is Markovian, meaning that the density matrix at time t determines completely how the system evolves at that time.

Examining equation (18) closely, we see that it is equation (17) with a bunch of extra terms added. To make some sense of (18), we can take a look at the expecatation values of Q_n and P_n and their time-evolution. The relevant equations are stated below, and are derived in appendix A.

$$\begin{aligned}\frac{d}{dt}\langle Q_n \rangle &= \langle P_n \rangle - \frac{1}{2}\Gamma_n \langle Q_n \rangle \\ \frac{d}{dt}\langle P_n \rangle &= -\Omega_n^2 \langle Q_n \rangle - \frac{1}{2}\Gamma_n \langle P_n \rangle\end{aligned} \tag{19}$$

The first term in each equation originates from the $[H_s, \rho]$ term in equation (18). These terms considered alone describe a harmonic oscillator. The second term in each equation only dampens Q_n and P_n, since Γ_n is never negative. From this system it is clear that Γ_n, which is equal to γk_n^2, controls the speed at which the oscillator decays to a state where $\langle Q_n \rangle = \langle P_n \rangle = 0$. Furthermore, when $k_n = 0$, D_n and Γ_n are both also zero. In this case, the normal mode n evolves as if no heat bath were present at all.

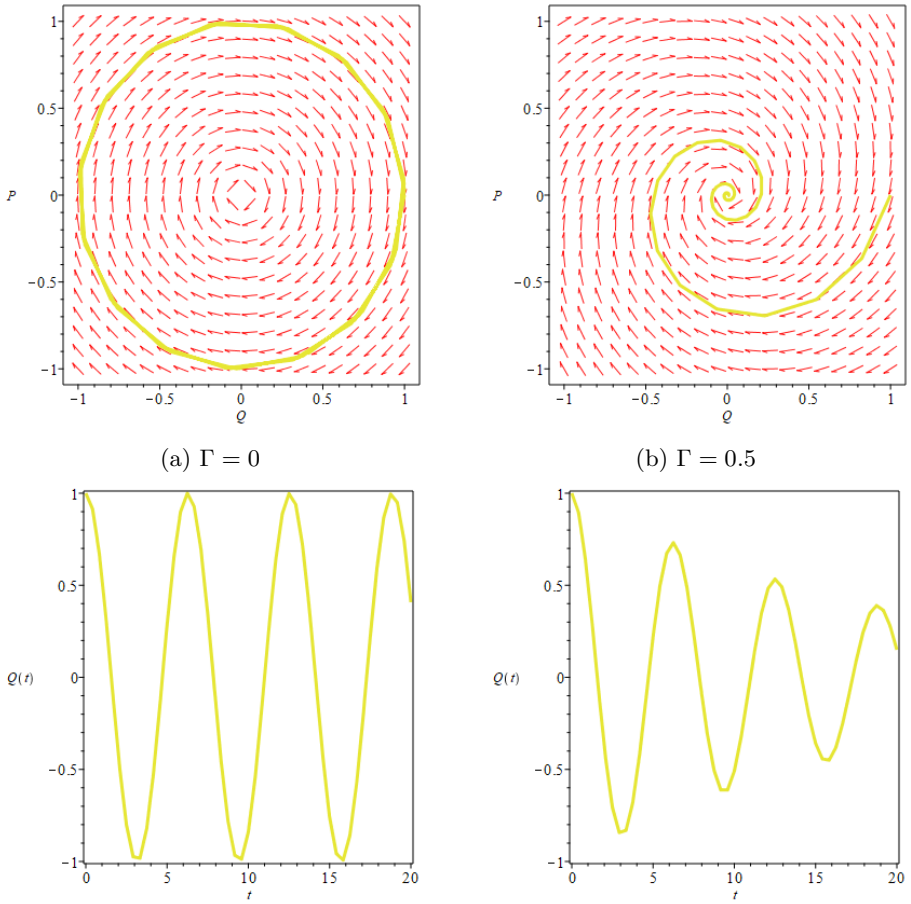

(a) $\Gamma = 0$ (b) $\Gamma = 0.5$

(c) $\Gamma = 0$ (d) $\Gamma = 0.5$

Figure 1: Phase diagram of $\langle Q \rangle$ and $\langle P \rangle$ (a and b) and time evolution of $\langle Q \rangle$ (c and d). $\Omega = 1$ in all figures. Initial conditions are $Q(0) = 1, P(0) = 0$. In all figures, t goes from 0 to 20.

Figure 1 shows how the expectation values of P and Q evolve in two scenarios. In the case of $\Gamma = 0$, the phase diagram shows that the evolution is periodic with period. In the case of $\Gamma = 0.5$, the expectation values quickly decay to 0.

We have seen that Γ_n greatly influences the rate at which a normal mode decays. Also, we have seen that for k_n close to zero, Γ_n and D_n are very small. This motivates the following definition.

Definition 1. *A noiseless cluster of a linearly coupled network of quantum harmonic oscillators is a normal mode which has $k_n = 0$. A quasi-noiseless cluster is a normal mode for which k_n is very close to* 0.

The definition of a quasi-noiseless cluster is somewhat ambiguous because of the phrase 'very close to'. In our case, we will perturb network matrices which have noiseless clusters. The strength of the perturbation is controlled with a parameter ϵ. We deem a normal mode a quasi-noiseless cluster if $k_n(\epsilon)$ is continuous in some interval around 0 and if $k_n(0) = 0$.

2.2 Experimental implementation of oscillator networks

A lot of research done on complex quantum networks has been theoretical in nature. Among others, complex quantum networks have been studied in the contexts of delocalization in networks with high clustering [4], phase transition of light [5], quantum random walks [6], and determining connectivity with a local probe [7]. However, not many physical experiments have been performed on these networks. This might be because creating an arbitrary physical complex quantum network seems to be a daunting task. It requires precise control over the interactions between all the nodes in the network, and the number of nodes must be sufficiently large if one wants to study networks with complex features.

However, Nokkola et al. have found a way to "create and control complex quantum networks with arbitrary topology in a single setup" [3]. They describe an optical setup which makes it possible to simulate the evolution of a complex quantum network of oscillators just like the ones in section 2.1.4. In this section, we describe how their setup works and how it could be applied to verify our results.

Before the setup can be created, some things must be calculated: first we must determine the network matrix M which is to be simulated, and choose a time t. This matrix could be a that of a network found 'in the wild' or it could be designed for some purpose. We orthogonally diagonalize M to find the normal modes of the network $Q = T_1^{-1}q$, $P = T_2^{-1}p$, and their frequencies Ω_i. Using these, we calculate the matrix S which maps the initial state of the normal mode quadratures $(Q(0), P(0))^\top$ to their final state $(Q(t), P(t))^\top$.

$$S = \begin{pmatrix} D^\Omega_{cos} & D^\Omega_{sin} \\ -D^\Omega_{sin} & D^\Omega_{cos} \end{pmatrix} \tag{20}$$

The equation above shows the block form of S. The i-th diagonal entry of D^Ω_{cos} is $cos(\Omega_i t)$, and D^Ω_{sin} is similar. With this matrix and the expressions $q = T_1 Q$,

$p = T_2 Q$, we compute the matrix S_v which maps $(q(0), p(0))^\top$ to $(q(t), p(t))$,

$$S_v = \begin{pmatrix} T_1 & 0 \\ 0 & T_2 \end{pmatrix} S \begin{pmatrix} T_1^{-1} & 0 \\ 0 & T_2^{-1} \end{pmatrix} \tag{21}$$

This final matrix S_v is then decomposed with a Bloch-Messiah decomposition into $S_v = R_1^\top \Delta^{sq} R_2$, where R_1 and R_2 are symplectic and orthogonal, and Δ^{sq} is a diagonal squeeze matrix. The matrices R_1, R_2 and Δ^{sq} determine the building blocks of the optical setup. For our purposes, the initial state of the system is unimportant, which means we can neglect the R_2 matrix.

2.2.1 Optical setup

In the experimental setup, a large number of entangled photons is produced with a mode-locked laser. These photons are then filtered and amplified by a frequency comb. The optical modes produced by this comb will perform the role of the normal mode oscillations.

When the optical modes have been generated, they need to be 'put through' the matrix S_v. First the modes must be squeezed according to Δ_{sq}. This is done by controlling the spectral shape of the frequency comb so that it decreases or increases the amplitude of the optical modes appropriately. The spectral shape of the comb is controlled by a parametric process, of which the parameters are optimized so that the comb closely matches Δ_{sq}.

The only thing left is to apply the matrix R_1 to the squeezed optical modes. This is done by modifying the basis along which the modes are measured. The measurement is performed by using homodyne detection with a local oscillator as described in [8]. By choosing the appropriate pulse shape for the local oscillator, any node in the network can be addressed.

2.2.2 Results of the simulation

Figure 2 shows two of the networks which Nokkola et. al. simulated. Figure 3 shows the result of their simulation of the networks. In the lower part of each box, the theoretical (brown line) and experimental (black line) mean number number of photons in each optical mode can be compared. The relative errors in the left and right boxes are 5.3% and 5% respectively. The mean number of photons $\langle n \rangle$ in the optical modes is directly analogous to n in equation (4), and determines the energy in each oscillator. The figure shows that the measured values of $\langle n \rangle$ are close to the theoretical values for every node in both networks. This gives reason to believe that the simulation approximates the network well.

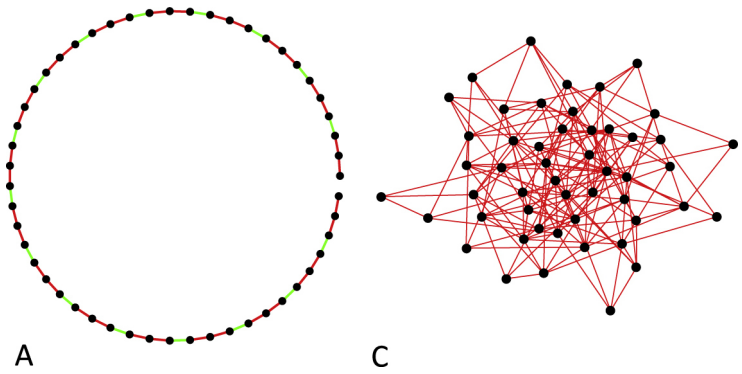

Figure 2: Two simulated networks from [3]. In network A, the green connections are 0.6 times as strong as the red connections. Network C is an Erdös-Renyi network with 50 nodes. All the connections in network C are equally strong.

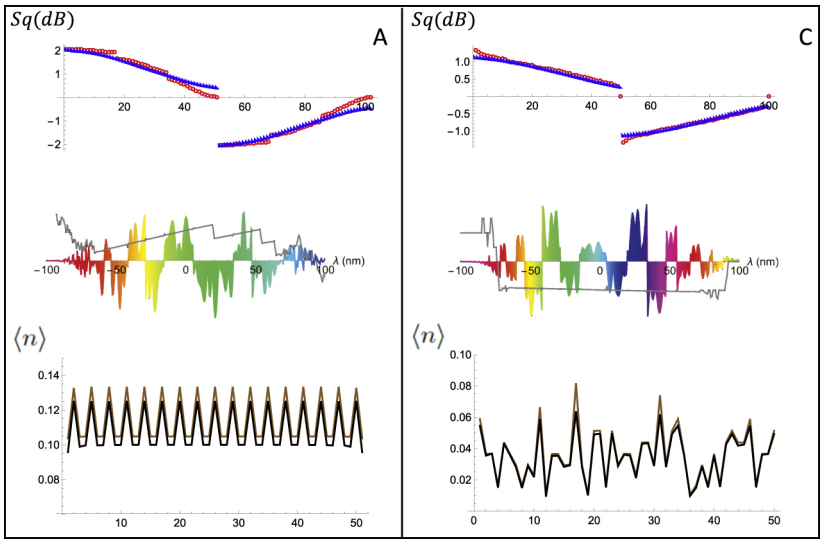

Figure 3: Results of optical simulation of two networks at $t = 50$ from [3]. The left and right boxes use networks A and C from figure 2 respectively. The top part of each box shows how well Δ_{sq} was approximated. In red are the diagonal entries of Δ_{sq}, in blue is the approximation by the parametric pump. The middle part of the boxes shows the pulse shape used to address the 26-th node. The color plot is the amplitude, and the grey line is the phase. The bottom part shows the theoretical (brown) and experimental (black) expectation values of the number of photons in each node

2.2.3 Application

The optical setup described is very versatile since the network matrix used is, in principle, arbitrary. The limiting factors are the number of optical modes available, how well Δ_{sq} can be approximated, and how well a given node can be addressed. The setup can even be used to simulate the thermodynamical heat bath described in section 2.1.5, since the bath also consists of harmonic oscillators.

We suspect therefore that it is possible to verify our results, in particular theorem 6, with this setup. We can imagine creating a network matrix with a sporadic noiseless cluster, and simulating perturbed versions of the network with the optical setup to see how quickly the noiseless cluster decays. A possible problem is that simulating the heat bath requires infinitely many optical modes. We are unsure if the number of optical modes available is large enough to approximate such a heat bath to a sufficient degree.

2.3 Random Networks and Symmetry

2.3.1 Erdös-Renyi networks

A random graph is a graph which is also a random variable. There are many ways to generate random graphs, but one of the simplest models is called the Erdős–Rényi (ER) model [12]. There are two versions of this model, but we will only consider the N, p version. This model has two parameters: N and p.

A graph is generated as follows: first, create an empty graph with N vertices. Then, for each possible edge, add the edge to the graph with probability p. Once all the edges have been considered, we are done.

Since we want to consider random networks of coupled oscillators, we must also have some way to translate a random graph to a network matrix. This can be done by considering the adjacency matrix A of the graph. This matrix will satisfy $A_{ij} = 1$ if there is an edge between nodes i and j, and 0 otherwise. Multiplying this matrix by the desired strength of the couplings λ, and setting the diagonal entries to $m\omega^2$, we obtain a network matrix which represents the graph.

Note that the previous section three extra parameters have been introduced. The model for random oscillator networks now has 5 parameters: p, N, ω, m and λ. However, the parameters m and ω do not affect the normal modes, since subtracting $m\omega^2$ from the diagonal of the network matrix only results in a global eigenvalue shift. Similarly, the λ parameter does not affect the normal modes, since multiplying a matrix by a constant leaves its eigenvectors unaffected. Regardless, we include them in the model.

Of course, many other methods of generating the network matrix are possible. The only restrictions are that the network matrix must be real symmetric, and that it the off-diagonal entries must be nonpositive.

2.3.2 Noiseless clusters from degeneracy

A common way through which noiseless clusters arise in random networks is via degeneracy. The following theorem shows how.

Theorem 1. *Let M be the network matrix (as described in section 2.1.4) of a network of oscillators. If M has two linearly independent eigenvectors with the same eigenvalue, then the network has a noiseless cluster.*

Proof. Suppose v and w are two linearly independent normal modes of the network with the same frequency ω. Express v and w in the node basis $\{x_1 ... x_n\}$, so that $v = \sum_{i=1}^{n} v_i x_i$ and $w = \sum_{i=1}^{n} w_i x_i$. Now consider the following linear combination of v and w:

$$u = v - \frac{\sum_{i=1}^{n} v_i}{\sum_{i=1}^{n} w_i} w \tag{22}$$

v and w are linearly independent, so u cannot be the zero vector. Furthermore, u is also a normal mode with frequency ω. The j-th coefficient of u is:

$$u_j = v_j - \frac{\sum_{i=1}^{n} v_i}{\sum_{i=1}^{n} w_i} w_j \tag{23}$$

Summing all the coefficient of u to compute k gives:

$$k = \sum_{j=1}^{n} u_j = \sum_{j=1}^{n} (v_j - \frac{\sum_{i=1}^{n} v_i}{\sum_{i=1}^{n} w_i} w_j) = \sum_{i=1}^{n} v_i - \frac{\sum_{i=1}^{n} v_i}{\sum_{i=1}^{n} w_i} \sum_{i=1}^{n} w_i = 0 \tag{24}$$

This shows that u is a normal mode of M of which the coefficients (in the standard basis) sum to zero, making it a noiseless subspace. □

2.3.3 Permutations

Degeneracies in the spectrum of M can be found by examining the symmetries of the network. These symmetries are permutations of the nodes which do not affect the dynamics of the system.

In our context, permutation are described by permutation matrices. A permutation can be associated with a linear transformation by letting it permute the basis vectors of a vector space. So if σ is a permutation of $\{1..n\}$, and $\{e_1...e_n\}$ is a basis of an n-dimensional vector space, then σ can be associated with the linear transformation P_σ which sends e_i to $e_{\sigma(i)}$.

If we express P in the basis $\{e_1...e_n\}$, then P has a exactly one 1 in every row and every column, and all the other entries are 0. Also, multiplication of matrices is compatible with the composition of permutations. If σ and ρ are permutations, then $P_\sigma(P_\rho e_i) = e_{\sigma(\rho(i))} = e_{\sigma\circ\rho(i)} = P_{\sigma\circ\rho} e_i$. Since matrices are uniquely defined by their action on the basis vectors and i was arbitrary, $P_\sigma P_\rho = P_{\sigma\circ\rho}$.

Symmetries in the network are described by permutation matrices which commute with M.

$$MP = PM \tag{25}$$

This equation effectively states that relabeling the nodes and applying the network dynamics is the same as first applying the dynamics and then relabeling the nodes.

It turns out that symmetries of this kind can very easily 'force' degenerate eigenvalues to be present. This is proven in the following theorem.

Theorem 2. *Let M be an n-dimensional hermitian matrix, and let ρ be a permutation of $1...n$. Let P be the permutation matrix corresponding to ρ. Suppose that P commutes with M, and that ρ has a cycle of length 3 or greater. Then M has a duplicate eigenvalue.*

To prove this theorem, we need the following lemma's. The proof of lemma 1 is fairly elementary and can be found in [17], for example.

Lemma 1. *Let ρ be a permutation written as a product of k disjoint cycles, and let l_i be the length of the i-th cycle of ρ. Let P be the permutation matrix corresponding to ρ. Then the eigenvalues of P are exactly*

$$\bigcup_{i=1}^{k} \{z \in \mathbb{C} | z^{l_i} = 1\} \tag{26}$$

Proof. Let let σ be an arbitrary cycle of ρ with length l. Then there are numbers n_k for $k \in \{1..l\}$ which σ permutes cyclically. Correspondingly, there are basis vectors vectors e_k which are permuted cyclically by P. Now consider the vector

$$v = \sum_{k=1}^{n} e_k \exp(2\pi i m k/l) \tag{27}$$

for any $m \in \{0..l-1\}$. Since P sends e_k to e_{k+1} (and e_l to e_1), Pv is the same as $\exp(2\pi i m/l)v$, and therefore the l-th roots of unity are eigenvalues of P.

In this way, we obtain l eigenvectors for each cycle of length l. Since the sum of the lengths of the disjoint cycles (including trivial ones) is equal to the dimension of the matrix, we have found all eigenvalues and eigenvectors. □

Lemma 2 is a basic result from linear algebra, which can be found in [10] or many other textbooks.

Lemma 2. *Let P and M be diagonalizable matrices in $\mathbb{C}^{n^2}$. Then if $PM = MP$, there exists a basis of $\mathbb{C}^n$ consisting of simultaneous eigenvectors of P and M.*

Now for the proof of the theorem. The first lemma explicitly shows that P is diagonalizable. Since $PM = MP$ by assumption, this means P and M are simultaneously diagonalizable (over $\mathbb{C}$) by lemma 2.

Assume by contradiction that M has *no* duplicate eigenvalues. Then the eigenspaces of M are all 1-dimensional, which forces every eigenvector of M to be an eigenvector of P. And since M is real and symmetric, is has real eigenvalues and eigenvectors. Therefore, P has an eigenbasis of purely real vectors. Also, P has at least one complex eigenvalue by lemma 1. The contradiction follows by noticing that P has only real entries, so it cannot have a real eigenbasis together with a complex eigenvalue.

Using theorems 1 and 2 together we conclude that all but the most trivial symmetries in the network necessarily give rise to noiseless clusters. However, these exact symmetries generally only occur in theoretically constructed networks. To figure out if approximate symmetries also give rise to approximate noiseless clusters, we need to find out what happens to the eigenvalues and eigenvectors of a matrix when it is slightly perturbed.

2.4 Perturbation Theory of Eigenvalue Problems

In this section, we state (without proof) some results from perturbation theory of finite-dimensional eigenvalue problems. For more information, including the proofs of the theorems, we refer to [11].

The first theorem concerns the eigenvalues of a perturbed matrix.

Theorem 3. *Let $A \in \mathbb{R}^{n^2}$ be symmetric with eigenvalues λ_i, and let $A(\epsilon)$ be a small perturbation of A which is symmetric for every ϵ. Then there exist functions $\lambda_i(\epsilon)$ which are power series in ϵ convergent for small $|\epsilon|$ for which $\lambda_i(0) = \lambda_i$.*

This theorem means that if we keep proper track of which eigenvalue is which, the eigenvalues of the perturbed matrix are 'close to' the eigenvalues of the original matrix.

The second theorem tells us about the eigenvectors of a perturbed matrix.

Theorem 4. *Let $A \in \mathbb{R}^{n^2}$ be symmetric. Suppose $A(\epsilon)$ is symmetric for every ϵ with $A(0) = A$, and suppose the entries of $A(\epsilon)$ are power series in ϵ convergent for small $|\epsilon|$. Suppose λ is an eigenvalue of A with multiplicity k. Then there exist power series*
$\lambda_i(\epsilon)$ for $i = 1..k$
$v_i^1(\epsilon)..v_i^n(\epsilon)$ for $i = 1..k$
convergent for small $|\epsilon|$ such that $(v_i^1(\epsilon), ..., v_i^n(\epsilon))^\top$ is an eigenvector of $A(\epsilon)$ with eigenvalue $\lambda_i(\epsilon)$.

This theorem tells us that for an analytic perturbation of A, the coefficients of the eigenvectors can be written as a power series in ϵ. Furthermore, theorems 3 and 4 permit us to calculate the eigenvalues and eigenvectors of a perturbed matrix to a first order approximation. The following derivation follows [9] roughly.

Suppose a hermitian n by n matrix A is given, along with the analytic permutation ϵB, where B is also hermitian. The eigenvalue problem we must solve is

$$(A + \epsilon B)v = \lambda v \tag{28}$$

Now, the preceding theorems allow us to write $v = v^0 + v^1\epsilon + v^2\epsilon^2 + ...$ and $\lambda = \lambda^0 + \lambda^1\epsilon + \lambda^2\epsilon^2 + ...$ Plugging this into equation (28) gives:

$$(A + \epsilon B)(v^0 + \epsilon v^1 + ...) = (\lambda^0 + \epsilon\lambda^1 + ...)(v^0 + \epsilon v^1 + ...) \tag{29}$$

Writing this out, collecting like terms of ϵ, and dropping any terms of order ϵ^2 or higher gives

$$Av^0 + \epsilon(Bv^0 + Av^1) = \lambda^0 v^0 + \epsilon(\lambda^1 v^0 + \lambda^0 v^1) \tag{30}$$

We can further simplify this equation by noting that $Av^0 = \lambda^0 v^0$ must hold. This can be seen by settings $\epsilon = 0$ in equation (29). Therefore, the first terms on both sides cancel out. Simplifying this further by dividing by ϵ on both sides results in the following expression:

$$Bv^0 + Av^1 = \lambda_1 v^0 + \lambda_0 v^1 \tag{31}$$

Next, take the inner product of (31) with v_0 from the left to get:

$$\langle v^0|Bv^0\rangle + \langle v^0|Av^1\rangle = \lambda^1\langle v^0|v^0\rangle + \lambda^0\langle v^0|v^1\rangle \tag{32}$$

Using the fact that A is hermitian, and that $Av^0 = \lambda_0 v^0$, this equation can be simplified to:

$$\lambda^1 = \langle v^0|Bv^0\rangle \tag{33}$$

We now work out an expression for v^1. Let v_i^0 be the set of eigenvectors of A, with corresponding eigenvalues λ_i.

Note that λ^i is the i-th order correction to the eigenvalue of $(A + \epsilon B)$, while λ_i is the i-th eigenvalue of A.

A is symmetric, so the v_i^0 vectors form a basis of $\mathbb{R}^n$. We can therefore write v^1 as a linear combination of the v_i^0 vectors.

$$v^1 = \sum_{i=1}^{n} c_i v_i^0 \tag{34}$$

We also rewrite equation (31).

$$(A - \lambda^0)v^1 = (\lambda^1 - B)v^0 \tag{35}$$

Now plug (34) into (35), and use that $Av_i^0 = \lambda_i v_i^0$.

$$\sum_{i=1}^{n} c_i(\lambda_i - \lambda^0)v_i^0 = (\lambda^1 - B)v^0 \tag{36}$$

Taking the inner product of v_m^0 with (36), and rewriting gives

$$c_m(\lambda_m - \lambda^0) = \lambda^1\langle v_m^0|v^0\rangle - \langle v_m^0|Bv^0\rangle \tag{37}$$

Since v^0 is an eigenvector of A, we can assume, without loss of generality, that $v^0 = v_n^0$ and $\lambda^0 = \lambda_n$. Substituting this in (37), as well as substutiting for λ^1 using (33) gives

$$c_m(\lambda_m - \lambda_n) = \langle v_n^0|Bv_n^0\rangle\langle v_m^0|v_n^0\rangle - \langle v_m^0|Bv_n^0\rangle \tag{38}$$

For $m = n$, the equation results in $0 = 0$. However, we are free to choose c_n to be equal to 0. If a vector a satisfies equation (35), then so does $a + cv^0$.

For $m \neq n$, we can solve for c_m.

$$c_m = \frac{\langle w_m | B w_n \rangle}{\lambda_m - \lambda_n} \tag{39}$$

Using this expression for c_m, we the final expression for the first-order correction to the eigenvector is:

$$v^1 = \sum_{m \neq n} \frac{\langle w_m | B | w_n \rangle}{\lambda_m - \lambda_n} w_m \tag{40}$$

2.4.1 Degeneracy

Note that care must be taken in the above derivation. Theorem 4 does not guarantee that any eigenvector of A will be analytically perturbed, only that there exist n eigenvectors for which this is the case. In the case of only 1-dimensional eigenspaces this is not a problem, because there is only one possible choice for the eigenvector basis (up to scalar multiplication). But when the multiplicity of λ is 2 or greater, expression (40) is only valid for the proper choice(s) of v^0. In this case, the extra terms where $\lambda_m = \lambda_n$ drop out of (40) exactly like the $c_n v_n^0$ term did.

3 Results

As we have seen, noiseless clusters can arise from various symmetries in ER networks. But there is no reason to assume all noiseless clusters are the result of symmetry. We have found that a distinction can be made between two types of noiseless clusters, and the types behave very differently in the presence of small perturbations.

3.1 Occurence of noiseless clusters in homogeneous networks

Cabot et al. [1] numerically determined the probabilities of noiseless clusters arising in Erdos-Renyi networks. We were able to reproduce their result, which is shown in figures 4 and 5. Only the left half of the figure is reproduced, since the figure must be symmetrical around $p = 0.5$. The following theorem indicates why.

Theorem 5. *If G is a network with a noiseless cluster, then the complementary network (which has edges exactly where G does not) also has a noiseless cluster.*

Proof. Denote the complement of G by G^c. Let M be the network matrix of G (as described in section 2.3.1). Then M has an eigenvector v with eigenvalue ω_n of which the coefficients in the standard basis sum to 0. Let M^c be the network matrix of G^c. Then $M^c = \lambda T - (m\omega^2 - \lambda)I - M$, where T is a matrix in which every entry is 1. Since the coefficients of v sum to 0, it must be true that $Tv = 0$. Therefore:

$$M^c v = \lambda T v - M v + (m\omega^2 - \lambda) I v = 0 - \omega_n v + (m\omega^2 - \lambda) v = (m\omega^2 - \omega_n - \lambda) v \quad (41)$$

and so v is also a normal mode of the complement of G, which makes v a noiseless cluster of G^c. □

From the figures, it is clear that noiseless clusters occur much more frequently for small N. This is likely because small networks are often symmetrical in some way, and therefore are likely to have noiseless clusters by theorems 1 and 2.

The larger networks with p close to zero have fewer edges, making them more likely to contain multiple small disconnected components. These smaller subnetworks can then contain noiseless clusters with a greater probability. The case for p close to 1 follows by symmetry.

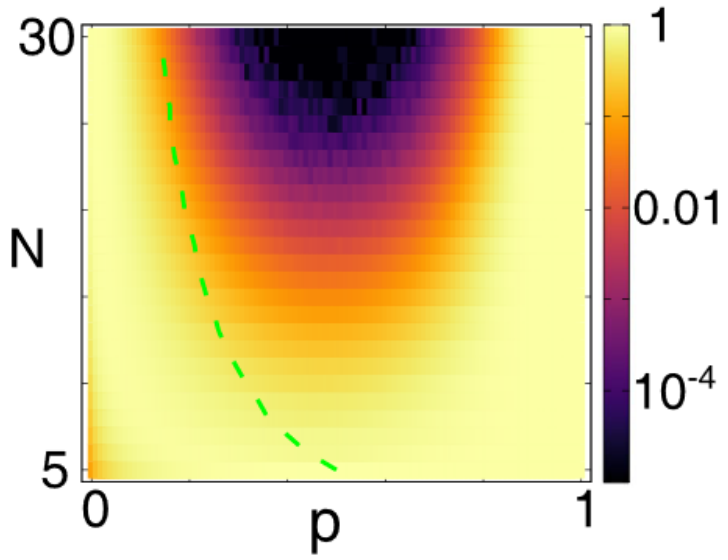

Figure 4: Frequency of ER networks with a noiseless cluster. N and p are the ER parameters. Figure created by Cabot et. al [1]

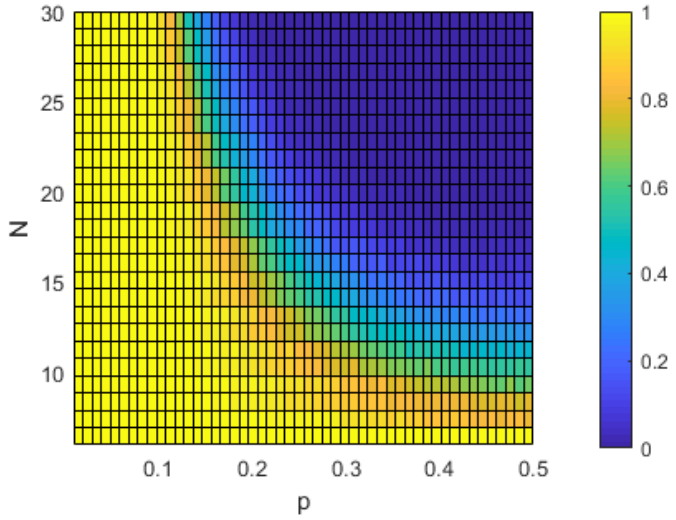

Figure 5: Reproduction of the left half of figure 4

3.2 Inhomogeneous networks

Instead of considering networks where the network matrix is exactly known, we now apply a perturbation to the strength of the couplings and or frequencies. The perturbation is modelled in the following way.

$$\omega_i = \omega_0 + \delta\omega_i \tag{42}$$

$$\lambda_{ij} = \lambda_{ji} = \lambda_0 + \delta\lambda_{ij} \tag{43}$$

In these equations, $\delta\omega_i$ and $\delta\lambda_{ij}$ are Gaussian random variables, and their variances are small compared to ω_0 and λ_0. We denote the variances of $\delta\omega_i$ and $\delta\lambda_{ij}$ by σ_ω and σ_λ.

The following sections apply to *any* network matrix where the entries are perturbed as specified above. If we imagine physically constructing a given network of oscillators, the perturbations can be interpreted as small deviations from the specification.

3.3 Effect of perturbations on noiseless clusters

Even when σ_ω and σ_λ are very small, the perturbations can have a profound influence on the presence of noiseless clusters. Firstly, the entries of any realisation of the network matrix are now continuous random variables. Since the eigenvalues of a matrix depend continuously on the entries of the matrix (see theorem 3), they too become continuous random variables. It is a basic probabilistic fact that the chance that two random variables are exactly equal is zero [13]. This means that the chance of duplicate eigenvalues is zero. Therefore, the method of finding noiseless subspaces described in section 2.3.2 in no longer applicable.

We now examine if networks with noiseless clusters become networks with quasi-noiseless clusters when they are perturbed. Unfortunately, this is not true in general, although it can occur. We identify three different outcomes, demonstrated by the following three networks.

$$N(\epsilon) = \begin{pmatrix} 1+\epsilon & 0 \\ 0 & 1 \end{pmatrix} \tag{44}$$

$$M(\epsilon) = \begin{pmatrix} 1 & \epsilon \\ \epsilon & 1 \end{pmatrix} \tag{45}$$

$$K(\epsilon) = \begin{pmatrix} 2\epsilon^2 - 4\epsilon + 3 & 1-\epsilon \\ 1-\epsilon & 2\epsilon^2 - 2\epsilon + 3 \end{pmatrix} \tag{46}$$

$N(\epsilon)$ represents a network of two uncoupled nodes, where the frequency of the first node is perturbed by ϵ. $M(\epsilon)$ represents a network of two uncoupled nodes, where the perturbation is a small coupling between the nodes. $K(\epsilon)$ represents a network where the coupling strength and the frequencies of the nodes are both

perturbed.

$N(0)$ and $M(0)$ are the identity, so by inspection $\frac{1}{\sqrt{2}}(1,-1)^\top$ is a noiseless cluster present in both unperturbed networks. This same vector is also an eigenvector of $K(0)$, as can be verified by inspection. All three networks have a noiseless cluster when unperturbed.

For $\epsilon \neq 0$ however, the eigenvalues of N are $1+\epsilon$ and 1, with eigenvectors $(1,0)^\top$ and $(0,1)^\top$ respectively. Neither of these normal modes are quasi-noiseless clusters. In fact, their values of k are independent of ϵ (as long as $\epsilon \neq 0$). Thus, even for the smallest nonzero perturbation, the noiseless cluster is completely destroyed.

The eigenvalues of $M(\epsilon)$ become $1+\epsilon$ and $1-\epsilon$ with eigenvectors $\frac{1}{\sqrt{2}}(1,1)^\top$ and $\frac{1}{\sqrt{2}}(1,-1)^\top$ respectively. The second of these is a noiseless cluster, regardless of ϵ.

Now consider $K(\epsilon)$. It can easily be verified that $v = (1, \epsilon - 1)^\top$ is an eigenvector of $K(\epsilon)$. The sum of the coefficients of the normalization of v is then $k = \frac{\epsilon}{\sqrt{1+(\epsilon-1)^2}}$. This expression is zero when $\epsilon = 0$, and is continuous and differentiable at 0. Therefore, for ϵ very small, the noiseless cluster of $K(\epsilon)$ becomes quasi-noiseless.

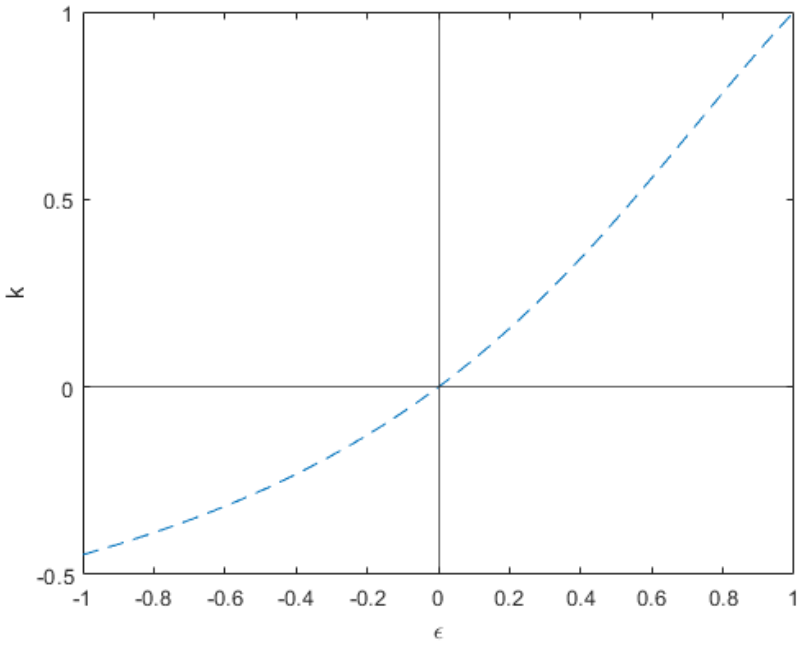

Figure 6: k plotted as a function of ϵ

Unfortunately, the behaviors of K and M are exceptions, while that of N is the rule. Numerical simulation confirms that networks with noiseless clusters arising exclusively from degeneracy of the spectrum show no signs of quasi-noiseless clusters when a small perturbation is present. These numerical results are described in section 3.5.

This is problematic for any physical applications, since no physical experiments can be calibrated to infinite precision. Therefore, noiseless clusters which arise from degeneracy are useless in practice.

3.4 Types of noiseless clusters

In our numerical simulation, we found that sometimes degenerate clusters occur when M has no degenerate eigenvalues. We now give these noiseless cluster a name, and specify how to identify them.

Definition 2. *Sporadic noiseless clusters*
Let M be a network matrix. A sporadic noiseless cluster of M is an eigenspace of M in which the coefficients of ***every*** *eigenvector sum to zero.*

This definition includes noiseless clusters which live in a 1-dimensional eigenspace.

Definition 3. *Degenerate noiseless cluster*
Let N be a network matrix. A degenerate noiseless cluster of N is a noiseless cluster which is ***not*** *sporadic.*

Looking again at the previous example, we now see that the noiseless clusters in $N(0)$ and $K(0)$ are degenerate, since the vector $\frac{1}{\sqrt{2}}(1,1)^\top$ is in the same eigenspace as $\frac{1}{\sqrt{2}}(1,-1)^\top$, but is not a noiseless cluster.

In the next section, we shall see that these types of noiseless clusters behave very differently when the network is perturbed. It is interesting that whether or not a noiseless cluster is degenerate or sporadic is only dependent on the *un*perturbed network matrix.

3.5 Perturbation of a degenerate noiseless cluster

To find out how the two types of noiseless clusters respond to perturbations, we simulated them numerically. This section describes what happened to the degenerate clusters.

Figure 7 was created in the following way.

1. Generate an ER networks with $p = 0.1$ and $N = 50$
2. Compute the network matrix M
3. Compute a perturbed version M' by adding an $N(0, 10^{-10})$ variables to every entry of M
4. Diagonalize M' and find the smallest k of its eigenvectors. Store k
5. Repeat 3-4 as many times as desired
6. Plot a histogram of the stored values of k

Figure 7 is a realization of just of one (arbitrary) network, but is representative of networks with only degenerate noiseless clusters. Other simulations gave distributions with the same general shape and with a mean value of k of the same order of magnitude.

Figure 8 shows the same simulation performed on a network which had no noiseless clusters of any type. Remarkably, the two figures look very similar. They have the same general shape, and the mean of the smallest k is within the same order of magnitude. By comparing many realization of the two figures, we concluded that there was no distinguishable difference between networks with a degenerate cluster and networks with no noiseless clusters. It appears that with even the smallest perturbation, a degenerate noiseless cluster is just as good as no noiseless cluster at all.

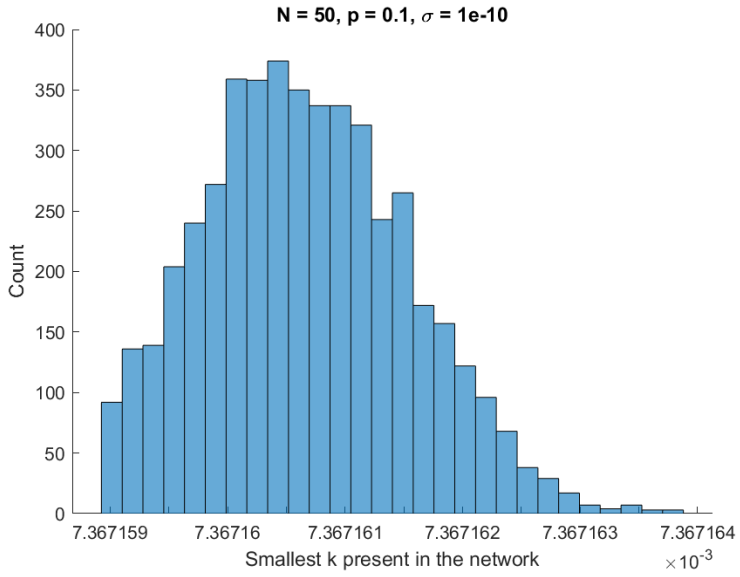

Figure 7: Histogram of smallest k after perturbation of a network which had only a degenerate noiseless cluster. The number of simulations was 5000.

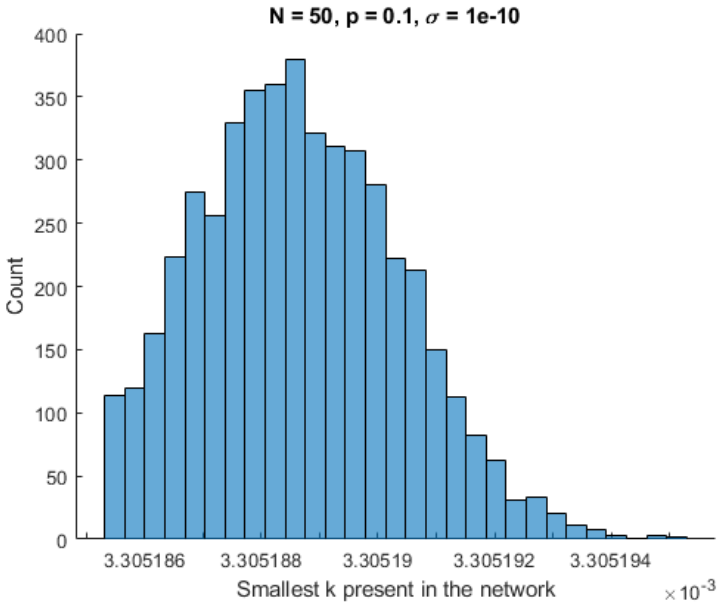

Figure 8: Histogram of smallest k after perturbation of a network which had no noiseless clusters. The number of simulations was 5000.

3.6 Perturbation of sporadic noiseless cluster

It turns out that a perturbation of a network with a sporadic noiseless cluster *is* guaranteed to produce a quasi-noiseless cluster. We back up this claim with numerical evidence, as well as the following theorem. Note that this theorem holds for *any* network matrix, not just those generated by an Erdös-Renyi model.

Theorem 6. *Let N be the network matrix of a network which has a sporadic normal mode. Let the coefficients of N are perturbed by normal random variables with mean 0 and standard deviation σ. Denote the normal modes of N by ψ_i, and denote their frequency by ω_i. Denote the sum of the coefficients of the n-th normal mode by k_n. Without loss of generality, assume the sporadic noiseless cluster is the n-th normal mode.*

Then the distribution of absolute value of the sum of the coefficients of the perturbed noiseless cluster is (to first order) a folded normal distribution with

$$\sigma_1^2 = \sigma^2 \sum_{m \neq n} (\frac{1}{\omega_n - \omega_m} k_m)^2 \tag{47}$$

Proof. We start using the equation for the perturbed eigenvector from section 3.5. Let H be the matrix with the perturbing entries. Write H^{xy} for the component in row x and column y of H. Then each H^{xy} is normally distributed with mean 0 and standard deviation σ.

$$\psi_n' = \sum_{m \neq n} \frac{\langle \psi_m | H | \psi_n \rangle}{\omega_n - \omega_m} \psi_m \tag{48}$$

Now sum over the coefficients of each term

$$k_n' = \sum_{m \neq n} \frac{\langle \psi_m | H | \psi_n \rangle}{\omega_n - \omega_m} k_m \tag{49}$$

Now split the inner product into its individual components. Denote by ψ^x the x-th component of ψ.

$$k_n' = \sum_{m \neq n} \frac{k_m}{\omega_n - \omega_m} \sum_x \sum_y \psi_m^x H^{xy} \psi_n^y \tag{50}$$

Interchange the summation and rearrange

$$k_n' = \sum_x \sum_y H^{xy} \sum_{m \neq n} \frac{\psi_m^x \psi_n^y}{\omega_n - \omega_m} k_m \tag{51}$$

Since each H^{xy} is $N(0, \sigma^2)$ distributed, each of the terms in the sum over x and y is also normally distributed, but with standard deviation $\sigma \sum_{m \neq n} \frac{\psi_m^x \psi_n^y}{\omega_n - \omega_m} k_m$.

The sum of all these terms is then also normally distributed (since the H^{xy}'s are independent). If we call the standard deviation of this distribution σ_1, then

$$\sigma_1^2 = \sum_x \sum_y (\sigma \sum_{m \neq n} \frac{\psi_m^x \psi_n^y}{\omega_n - \omega_m} k_m)^2 \tag{52}$$

We now expand the quadratic term using the multinomial formula. We split the quadratic terms and the cross-terms into two seperate sums.

$$\sigma_1^2 = \sigma^2 (\sum_x \sum_y (\sum_{m \neq n} (\frac{\psi_m^x \psi_n^y}{\omega_n - \omega_m} k_m)^2 + 2 \sum_{(i \neq n, j \neq n, i \neq j)} \frac{\psi_i^x \psi_n^y \psi_j^x \psi_n^y}{(\omega_n - \omega_i)(\omega_n - \omega j)} k_i k_j)) \tag{53}$$

Rearranging the terms, and interchanging the summation, we can rewrite the second sum to

$$2\sigma^2 \sum_{(i \neq n, j \neq n, i \neq j)} \frac{1}{(\omega_n - \omega_i)(\omega_n - \omega j)} k_i k_j \sum_y (\psi_n^y)^2 \sum_x \psi_i^x \psi_j^x \tag{54}$$

Now notice that the rightmost part is just the inner product between ψ_i and ψ_j. But since they are both eigenvectors of a hermitian matrix, this inner product is zero. This causes the whole sum to vanish. Therefore, σ_1 becomes

$$\sigma_1^2 = \sigma^2 \sum_x \sum_y \sum_{m \neq n} (\frac{\psi_m^x \psi_n^y}{\omega_n - \omega_m} k_m)^2 \tag{55}$$

Now interchange the summation and rearrange once more to get

$$\sigma_1^2 = \sigma^2 \sum_{m \neq n} (\frac{k_m}{\omega_n - \omega_m})^2 \sum_x (\psi_m^x)^2 \sum_y (\psi_n^y)^2 \tag{56}$$

Notice that the last part of the equation is just the ℓ_2 norms of ψ_m and ψ_n. Since ψ_m and ψ_n are normalized, this is always 1. We are therefore left with

$$\sigma_1^2 = \sigma^2 \sum_{m \neq n} (\frac{k_m}{\omega_n - \omega_m})^2 \tag{57}$$

Since k'_n is normally distributed with this standard deviation, the result follows by taking the absolute value of k'_n. □

Theorem 6 has two important implications. Firstly, it is proof that a sporadic noiseless cluster becomes quasi-noiseless when the network is perturbed slightly. This means we can find or construct a network which contains a sporadic noiseless cluster and, unlike in the case of a degenerate noiseless cluster, be assured that a physical realization of the network (which will have slight perturbations) contains a normal mode with a long decoherence time.

Secondly, for a given network with a sporadic noiseless cluster, we can determine

exactly how resistant it is to a perturbation. This can be evaluated using the ratio between σ_1^2 and σ^2. We will call this ratio the structure factor and denote it by S, since it is determined by the structure of the network.

$$S = \sum_{m \neq n} \left(\frac{k_m}{\omega_n - \omega_m}\right)^2 \tag{58}$$

In a way, S represents how strongly a perturbation is amplified by the network. From equation 58 it is clear that S is determined by the eigenfrequencies of the network ω_i and by the k's of the other normal modes. Apparently, the normal modes which are close in frequency to the noiseless mode have a big influence on S, whereas the modes with a big frequency difference have a small impact.

Since the result of theorem 6 is only valid to first order in perturbation theory, we verify it using numerical simulations. Figure 9 shows the result of the exact same simulation as those used to produce figures 7 and 8, but performed on a network with a sporadic noiseless cluster. The figure demonstrates that the half-normal distribution fits neatly onto the observed data.

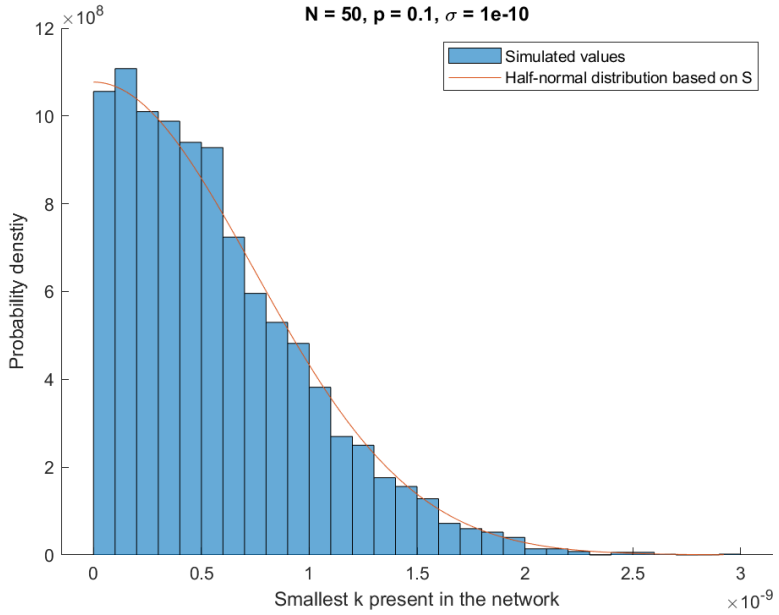

Figure 9: Smallest k after perturbation of a network which had one or more sporadic noiseless clusters. The number of simulations was 10000.

A big contrast can be seen between figure 9 on the one hand, and figures 7 and 8 on the other hand. Firstly, the shape of the distributions is completely different. Figure 9 is well-fitted by a half-normal distribution, while figures 7 and

8 more closely resemble some type of skewed normal distribution. Furthermore, the observed values of $|k|$ for the degenerate clusters are roughly 6 orders of magnitudes greater than those of the sporadic clusters.

3.7 An upper bound on S in Erdös-Renyi networks

Since there are only a finite number of possible (homogeneous) ER networks with N nodes, there are a finite number of possible values which ω_i can take for each N. This means there exists a lower bound on $|\omega_n - \omega_m|$, and thus there is an upper bound on S.

First, we bound k_m by considering that the normal mode vector of the network must be normalized. We can then see that for a normal mode v with components v_i in a network with N oscillators the following holds.

$$k = |\sum_{i=1}^{N} v_i| \leq \sum_{i=1}^{N} |v_i| \leq \sqrt{N} \sum_{i=1}^{N} |v_i|^2 = \sqrt{N} \tag{59}$$

where we have used a basic inequality from real analysis [14].

The lower bound on $|\omega_n - \omega_m|$ is much more difficult. The best we were able to find is a theorem about the distance between the roots of polynomials.

Theorem 7. [16] *Let $P(X)$ be a separable polynomial with integer coefficients of degree $n \geq 2$. For any distinct zeros α and β of $P(X)$ it holds that*

$$|\alpha - \beta| \geq \sqrt{3}(n+1)^{-(2n+1)/2} H(P)^{-n+1} \tag{60}$$

In this equation $H(P)$ is the height *of the polynomial, which is defined as the maximum of the absolute value of the coefficients of the polynomial.*

Since all the oscillators in our ER network have the same frequency and mass, we may just as well set all diagonal entries to 0, since this shifts all (eigen-)frequencies equally. Furthermore, the off-diagonal entries of the network matrix are either $-\lambda$ or 0. This means we can factor out $-\lambda$ and consider a matrix in which the entries are either 1 or 0, and multiply the bound by $-\lambda$ afterwards. It can easily be verified that the characteristic polynomial of such a matrix can only have coefficients -1, 0, or 1. Therefore, $H(p) = 1$ for this polynomial.

The characteristic polynomial is only separable if all eigenvalues of the network matrix are distinct. If this is not the case, we cannot apply theorem 7. Therefore, the upper bound on S is only valid for networks with no degenerate eigenvalues.

We now put everything together.

$$\begin{aligned} S &= \sum_{m \neq n} \left(\frac{k_m}{\omega_n - \omega_m}\right)^2 \\ &\leq \sum_{m \neq n} \left(\frac{\sqrt{N}}{\lambda\sqrt{3}(N+1)^{-(2N+1)/2}}\right)^2 \\ &\leq \frac{(N-1)N}{3\lambda^2}(N+1)^{2N+1} \end{aligned} \tag{61}$$

Unfortunately, this bound is not very helpful, since it grows as N^N. By the time $N = 10$, the upper bound is already $2.2 * 10^{23}\lambda^{-2}$. The bound on $\omega_n - \omega_m$ is responsible for this, because of that is where the N^N term originates. We were unable to find a better lower bound for the seperation of the eigenvalues. In our simulations, S never even got close to this bound.

4 Conclusion

In this thesis we have investigated noiseless clusters in complex quantum networks. A network of quantum harmonic oscillators can be described in terms of its normal modes and frequencies. When all nodes in the network are coupled to a common heat bath, the normal modes decay at different rates. The rate of their decay is determined by a k, which is the sum of the components of the normalized normal mode vector when described in node coordinates. When $k = 0$ for a certain normal mode, the network is said to have a noiseless cluster. When $|k|$ is very small, the network has a quasi-noiseless cluster.

We have shown that there are two different types of noiseless clusters. A *degenerate* cluster is one that arises from a duplicate eigenfrequency of the network. If a network has a degenerate eigenfrequency, the normal modes corresponding to that frequency can be combined to form a normal mode with $k = 0$. We have demonstrated that when the network is slightly perturbed, these noiseless clusters do not transform into quasi-noiseless clusters. We have numerically shown that networks with only degenerate noiseless clusters and networks without any noiseless clusters are indistinguishable when looking at the smallest values of $|k|$ present in the perturbed network. We therefore conclude that degenerate noiseless clusters are unusable in any physical experiment, since experimental variables can in general never be *exactly* measured or controlled.

We have called the other kind of noiseless cluster *sporadic*. Sporadic noiseless clusters do become quasi-noiseless when the network is slightly perturbed. We have demonstrated this numerically, and formulated a theorem which shows how $|k|$ is distributed when the coupling strengths and frequencies of the network are perturbed by i.i.d. Gaussian random variables. The distribution of $|k|$ depends only the variable S, which is determined by the values of k of the other normal modes, and the difference in frequency between the other normal modes and the sporadic noiseless cluster.

$$S = \sum_{m \neq n} \left(\frac{k_m}{\omega_n - \omega_m}\right)^2$$

When S is very small, the perturbed values of $|k|$ are also very small. A limitation on our finding is that the theorem is only applicable if the perturbation of the coupling strengths and of the frequencies of the nodes is equal in size. In practice, it is unlikely that the perturbations in these physically different variables have the same distribution.

We have also determined an upper bound on the value of S for Erdös-Renyi networks of size N with no degenerate normal modes. However, this upper bound blows up incredibly quickly, as it contains of term in the order of N^N.

References

[1] Albert Cabot, Fernando Galve, Víctor M. Eguíluz, Konstantin Klemm, Sabrina Maniscalco, and Roberta Zambrini, *Unveiling noiseless clusters in complex quantum networks*, npj Quantum Information **4** (2018).

[2] Gonzalo Manzano, Fernando Galve, Gian Luca Giorni, Emilio Hernández-García, and Roberta Zambrini, *Synchronization, quantum correlations and entanglement in oscillator networks*, Scientific Reports **3** (2013).

[3] J. Nokkola, F. Arzani, R. Zambrini, S. Maniscalco, J. Piilo, N. Treps, and V. Parigi, *Reconfigurable optical implementation of quantum complex networks*, New Journal of Physics **20** (May 9, 2018).

[4] Lukas Jahnke, Jan W. Kantelhardt, Richard Berkovits, and Shlomo Havlin, *Wave Localization in Complex Networks with High Clustering*, Physical Review Letters **101**.

[5] Arda Halu, Silvano Garnerone, Alessandro Vezzani, and Ginestra Bianconi, *Phase transition of light on complex quantum networks*, Physical Review E **87** (February 7, 2013).

[6] Oliver Mülken and Alexander Blumen, *Continuous-Time Quantum Walks: Models for Coherent Transport on Complex Networks*, Physical Reports **502** (May 2011).

[7] Johannes Nokkola, Sabrina Maniscalko, and Jyrki Piilo, *Local probe for connectivity and coupling strength in quantum complex networks*, Scientific Reports **8** (2018).

[8] Y. Cai, J. Roslund, G. Ferrini, F. Arzani, X. Xu, C. Fabre, and N. Treps, *Multimode entanglement in reconfigurable graph states using optical frequency combs*, Nature Communications **8** (2010).

[9] David J. Griffiths, *Introduction to Quantum Mechanics*, 2nd ed., Cambridge University Press, 2018.

[10] Lorenzo Sadun, *Applied Linear Algebra*: *The Decoupling Principle*, 2nd ed., American Mathematical Society, 2008.

[11] Franz Rellich, *Perturbation Theory of Eigenvalue Problems*, Gordon and Breach Science Publishers, 1969.

[12] Albert Barabási, *Network Science*, 2015. Online edition, retrieved from `http://networksciencebook.com/`.

[13] Geoffrey Grimmett and Dominic Welsh, *Probability*: *An Introduction*, 2nd ed., Oxford University Press, 2017.

[14] N.L. Carothers, *Real Analysis*, Cambridge University Press, 2006.

[15] Daniel Manzano, *A short introduction to the Lindblad Master Equation*, AIP Advances **10** (2020).

[16] K. Mahler, *An inequality for the discriminant of a polynomial*, Michigan Mathematical Journal **11** (1964).

[17] M.I. García-Planas and M. D. Magret, *Eigenvalues and eigenvectors of monomial matrices*, June 8, 2015. Retrieved from `https://core.ac.uk/download/pdf/41824776.pdf`.

Appendix: Derivaton of expectation values

In this appendix, we derive equation (19) from the Lindblad Master equation (18) of the system. We work in the normal mode coordines, i.e. Q_n and P_n are the position and momentum operators of the n-th normal mode. We also set $\hbar = 1$.

We begin by stating the commutation relations of the normal mode coordinates.

$$\begin{aligned} [Q_n, P_m] &= i\delta_{mn} \\ [Q_n, Q_m] &= 0 \\ [P_n, P_m] &= 0 \end{aligned} \tag{62}$$

The starting point of the derivation is equation (18), repeated here.

$$\begin{aligned} \frac{d\rho(t)}{dt} =& -i[H_s, \rho] \\ & - \frac{i}{4}\sum_{i=1}^{N} \Gamma_i([Q_i, \{P_i, \rho\}] - [P_i, \{Q_i, \rho\}]) \\ & - \frac{1}{4}\sum_{i=1}^{N} D_i([Q_i, [Q_i, \rho]]) - \frac{1}{\Omega_i^2}[P_i, [P_i, \rho]]) \end{aligned} \tag{63}$$

In this equation H_s is the hamiltonian of the system of oscillators. In normal mode coordinates, this hamiltonian is

$$H_s = \frac{1}{2}\sum_{i=1}^{N}(P_n^2 + \Omega_n^2 Q_n^2) \tag{64}$$

We first show that for a time-independent operator T, $\frac{d}{dt}\langle T\rangle = tr(T\frac{d\rho}{dt})$.

$$\begin{aligned} &\frac{d}{dt}\langle T\rangle = \frac{d}{dt}tr(T\rho) = \frac{d}{dt}\sum_{i=1}^{N}\langle\psi_i|T\rho|\psi_i\rangle = \sum_{i=1}^{N}\frac{d}{dt}\langle\psi_i|T\rho|\psi_i\rangle \\ &= \sum_{i=1}^{N}\langle\psi_i|\frac{d}{dt}(T\rho)|\psi_i\rangle = \sum_{i=1}^{N}\langle\psi_i|T(\frac{d}{dt}(\rho)|\psi_i\rangle = tr(T\frac{d\rho}{dt}) \end{aligned} \tag{65}$$

In this derivation, we have used the fact that $\frac{dT}{dt} = 0$, as well as the $\frac{d\psi_i}{dt} = 0$, since the ψ_i are stationary basis states of the relevant Hilbert space.

Since the trace is linear, we can compute the terms separately and add everything up afterwards. We may also cyclically permute any term we like, since the trace is invariant under cyclic permutation.

We start with the first term of equation (63) for $tr(Q_n\frac{d\rho}{dt})$. For readability,

we omit the taking of the trace from now on. From now on the '=' symbol must be interpreted as 'has the same trace' until we specify otherwise.

$$\begin{aligned} &-iQ_n[H_s,\rho] = -i(Q_nH_s\rho - Q_n\rho H_s) = -i(Q_nH_s\rho - H_sQ_n\rho) \\ &= -i[Q_n,H_s]\rho = -i[Q_n,\frac{1}{2}P_n^2]\rho = (\frac{-i}{2}[Q_n,P_n]P_n + P_n[Q_n,P_n])\rho \\ &= \frac{-i}{2}(iP_n + iP_n) = P_n\rho \end{aligned} \tag{66}$$

The first term for $tr(P_n\frac{d\rho}{dt})$ is very similar, so we skip to the part where the branching occurs.

$$\begin{aligned} &-iP_n[H_s,\rho] = ... = -i[P_n,H_s]\rho = -i[P_n,\frac{1}{2}\Omega_n^2Q_n^2]\rho \\ &= \frac{-i\Omega_n^2}{2}[P_n,Q_n]Q_n + Q_n[P_n,Q_n]\rho = \frac{-i\Omega_n^2}{2}(-iQ_n + -iQ_n)\rho \\ &= -\Omega_n^2Q_n\rho \end{aligned} \tag{67}$$

We derive the second and third term for Q_n and P_n simultaneously. Let T be either Q_n or P_n.

We first consider the third term of equation (63). We only consider the part with Q_i, since the derivation is also valid when P_i is substituted for Q_i.

$$\begin{aligned} &T[Q_i,[Q_i\rho]] = T[Q_i,(Q_i\rho - \rho Q_i)] \\ =&TQ_iQ_i\rho - TQ_i\rho Q_i - TQ_i\rho Q_i + T\rho Q_iQ_i \\ =&(TQ_iQ_i - Q_iTQ_i - Q_iTQ_i + Q_iQ_iT)\rho \\ =&([T,Q_i]Q_i + Q_i[Q_i,T])\rho \\ =&([T,Q_i]Q_i - Q_i[T,Q_i])\rho = 0 \end{aligned} \tag{68}$$

The final step is valid because $[T,Q_i]$ is a constant (either 0, -1 or 1), and so the terms cancel. Therefore, the third term of (63) drops out completely.

Now to compute the second term of equation (63). We first show all the terms with $i \neq n$ evaluate to zero. In this case T commutes with Q_i and P_i. Again, we only consider the first part of the second term of (63). The second part follows by swapping P_i and Q_i in the derivation.

$$\begin{aligned} &T[Q_i,\{P_i,\rho\}] = TQ_iP_i\rho + TQ_i\rho P_i - TP_i\rho Q_i - T\rho P_iQ_i \\ &= T(Q_iP_i + P_iQ_i - Q_iP_i - P_iQ_i)\rho = 0 \end{aligned} \tag{69}$$

Now consider the case $i = n$. For now, we leave out the constant $\frac{-i}{4}\Gamma_i$ for

readability.

$$
\begin{aligned}
&T[Q_i,\{P_i,\rho\}]-T[P_i,\{Q_i,\rho\}]\\
&=T(Q_iP_i\rho+Q_i\rho P_i-P_i\rho Q_i-\rho P_iQ_i-P_iQ_i\rho-P_i\rho Q_i+Q_i\rho P_i+\rho Q_iP_i)\\
&=(TQ_iP_i+P_iTQ_i-Q_iTP_i-P_iQ_iT-TP_iQ_i-Q_iTP_i+P_iTQ_i+Q_iP_iT)\rho\\
&=(2P_iTQ_i-2Q_iTP_i+TQ_iP_i-P_iQ_iT-TP_iQ_i+Q_iP_iT)\rho\\
&=(2P_iTQ_i-2Q_iTP_i+T[Q_i,P_i]+[Q_i,P_i]T)\rho\\
&=(2P_iTQ_i-2Q_iTP_i+2iT)\rho\\
&=2(P_iTQ_i-Q_iTP_i+iT)\rho
\end{aligned}
\tag{70}
$$

We bifurcate depending on T, starting with $T=Q_i$:

$$
\begin{aligned}
&=2(P_iQ_iQ_i-Q_iQ_iP_i+iQ_i)\rho\\
&=2([P_i,Q_iQ_i]+iQ_i)\rho\\
&=2([P_i,Q_i]Q_i+Q_i[P_i,Q_i]+iQ_i)\rho\\
&=2(-iQ_i-iQ_i+iQ_i)\rho=-2iQ_i
\end{aligned}
\tag{71}
$$

The case $T=P_i$ goes similarly:

$$
\begin{aligned}
&=2(P_iP_iQ_i-Q_iP_iP_i+iP_i)\rho\\
&=2([P_iP_i,Q_i]+iP_i)\rho\\
&=2(P_i[P_i,Q_i]+[P_i,Q_i]P_i+iP_i)\rho\\
&=2(-iP_i-iP_i+iP_i)\rho=-2iP_i\rho
\end{aligned}
\tag{72}
$$

In both cases, we ended up with $-2iT\rho$. We still have to multiply with $\frac{i\Gamma_i}{4}$, which leaves us with $-\frac{\Gamma_i}{2}T\rho$.

We now put everything together. From this point, the '=' symbol should be interpreted in the ordinary sense.

$$
\begin{aligned}
\frac{d}{dt}\langle Q_n\rangle &= tr(P_n\rho)-tr(\frac{\Gamma_n}{2}Q_n)=\langle P_n\rangle-\frac{\Gamma}{2}\langle Q_n\rangle\\
\frac{d}{dt}\langle P_n\rangle &= tr(-\Omega_n^2Q_n\rho)-tr(\frac{\Gamma_n}{2}P_n)=-\Omega_n^2\langle Q_n\rangle-\frac{\Gamma}{2}\langle P_n\rangle
\end{aligned}
\tag{73}
$$

This concludes the derivation.